



THE UNIVERSITY *of* EDINBURGH

Edinburgh Research Explorer

Low coordinate NHC-Zinc-Hydride Complexes Catalyze Alkyne C-H Borylation and Hydroboration using Pinacolborane

Citation for published version:

Procter, RJ, Uzelac, M, Cid, J, Rushworth, PJ & Ingleson, MJ 2019, 'Low coordinate NHC-Zinc-Hydride Complexes Catalyze Alkyne C-H Borylation and Hydroboration using Pinacolborane', *ACS Catalysis*.
<https://doi.org/10.1021/acscatal.9b01370>

Digital Object Identifier (DOI):

[10.1021/acscatal.9b01370](https://doi.org/10.1021/acscatal.9b01370)

Link:

[Link to publication record in Edinburgh Research Explorer](#)

Document Version:

Peer reviewed version

Published In:

ACS Catalysis

General rights

Copyright for the publications made accessible via the Edinburgh Research Explorer is retained by the author(s) and / or other copyright owners and it is a condition of accessing these publications that users recognise and abide by the legal requirements associated with these rights.

Take down policy

The University of Edinburgh has made every reasonable effort to ensure that Edinburgh Research Explorer content complies with UK legislation. If you believe that the public display of this file breaches copyright please contact openaccess@ed.ac.uk providing details, and we will remove access to the work immediately and investigate your claim.



Low coordinate NHC-Zinc-Hydride Complexes Catalyze Alkyne C-H Borylation and Hydroboration using Pinacolborane

Richard. J. Procter^{§†}, Marina Uzelac^{§§}, Jessica Cid[†], Philip J. Rushworth[‡], Michael J. Ingleson^{§*}

[§] School of Chemistry, University of Edinburgh, Edinburgh, EH9 3FJ, UK

[†] School of Chemistry, University of Manchester, Manchester, M13 9PL, UK.

[‡] Research and Development, GlaxoSmithKline, Gunnels Wood Road, Stevenage SG1 2NY, U.K.

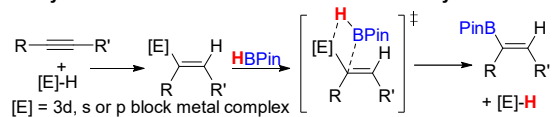
ABSTRACT: Organozinc compounds containing sp , sp^2 and sp^3 C-Zn moieties undergo transmetalation with pinacolborane (HBPin) to produce Zn-H species and organoboronate esters (RBPIn). This Zn-C/H-B metathesis step is key to enabling zinc catalyzed borylation reactions, with it used in this work to develop both terminal alkyne C-H borylation and internal alkyne hydroboration. These two conversions can be combined in one-pot to achieve the zinc catalyzed conversion of terminal alkynes to 1,1-diborylated alkenes without isolation of the sensitive (to protodeboration) alkynyl boronate ester intermediates. Mechanistic studies involving the isolation of intermediates, stoichiometric experiments and DFT calculations all support mechanisms involving organozinc species that undergo metathesis with HBPin. Furthermore, zinc catalyzed hydroboration can proceed via a hydrozincation step, which does not require any exogenous catalyst in contrast to all previously reported alkyne hydrozincations. Bulky *N*-heterocyclic carbenes (NHCs) are key for effective catalysis as the NHC steric bulk enhances the stability of NHC-Zn species present during catalysis and provides access to low coordinate (NHC)Zn-H cations that are electrophilic yet Brønsted basic. This work provides an alternative approach to access synthetically desirable pinacol-organoboronate esters using earth abundant metal based borylation catalysts.

Keywords: borylation; zinc; hydrides; *N*-heterocyclic carbene; homogeneous catalysis

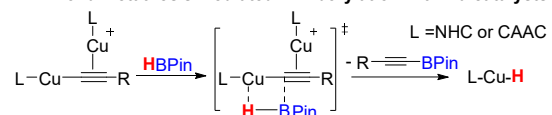
Introduction

The considerable utility of organoboranes has made them ubiquitous in synthesis and this provides a continued impetus to develop new routes to form C-B bonds.¹ Hydroboration and C-H borylation of hydrocarbons using commercial boranes, particularly HBPin / B₂Pin₂, represent efficient routes to C-B bonds.^{1b,2} Noble metal based catalysts have dominated this area and borylation methodologies now exist that are extremely powerful.^{1b,3} The replacement of noble metals with base metals that are earth abundant (e.g. Fe, Cu, Zn, Al), is desirable.⁴ However, catalysts based on base metals often react via distinct mechanisms to noble metals due to different propensities to undergo two electron redox steps. For base metal catalyzed borylation metathesis steps at a single redox state are often crucial (Figure 1A and B). While recent progress has been made in developing earth abundant metal based catalysts for alkyne hydroboration (Figure 1A),⁵ there are fewer examples of earth abundant metal based catalysts for C-H borylation.^{3c,6} Notable exceptions include NHC stabilized Fe and Cu catalysts for arene and alkyne C-H borylation, respectively (Figure 1B). However, most catalysts can only effect one step, hydroboration or C-H borylation, therefore a single earth abundant metal based catalyst that enables both alkyne C-H borylation and hydroboration would be highly desirable. For example, this would represent a useful catalytic conversion for converting terminal alkynes into diborylated alkenes.⁷ This conversion is of topical interest as the products are highly useful, however it should be noted that forming 1,1-diborylated alkenes from terminal alkynes is rare and much less common than the formation of the 1,2-isomers.⁸ Indeed, to the best of our knowledge, it is limited to two reports using either an iridium or a cobalt based catalyst.⁷ While highly notable work, Ir and Co have drawbacks with both having extremely low permitted

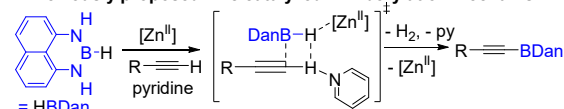
A: Hydrometalation / σ -bond Metathesis mediated hydroboration



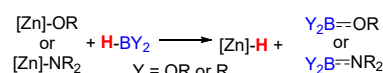
B: σ -Bond Metathesis mediated C-H borylation with Cu catalysts



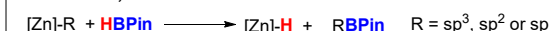
C: Previously proposed zinc catalyzed C-H borylation mechanism



D: Established Zn-H bond forming metathesis reactions



E: This work, stoichiometric Zn-R/HBPin metathesis demonstrated



This work: catalytic alkyne C-H borylation and hydroboration

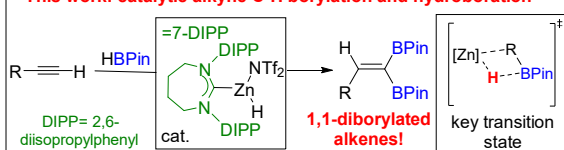


Figure 1 A-D select relevant previous work. E, inset this work demonstrating Zn-R/H-BPin transmetalation and zinc catalyzed C-H borylation and hydroboration for formation of 1,1-diborylated alkenes.

daily exposures (PDE) as defined by the European Medicines Agency,⁹ while Ir is also of low abundance. Thus the development of a catalyst based on a metal with a high PDE¹⁰ and high natural abundance that performs C-H borylation and hydroboration enabling formation of 1,1-diborylated alkenes from terminal alkynes would be significant.

As part of our ongoing interest in catalyzed C-H borylation¹¹ and using zinc complexes for σ bond formation we targeted zinc catalyzed C-B bond formation.¹² In previously reported base metal borylation catalysis a metal hydride is often an on cycle species generated concurrently with the desired organoborane via a σ -bond metathesis step between HBPIn and an organometallic species (e.g. Figure 1A and B). Notably to the best of our knowledge, the analogous metathesis reaction of organozinc and hydroborane species to form a zinc hydride and an organoborane has not been reported. Indeed, the only reported zinc catalyzed C-H borylation, that we are aware of,¹³ is of terminal alkynes using 1,8-naphthalene-diaminato-borane (HBDan), to afford alkynyl-BDan (Figure 1C). Notably, the more mainstream reagent, HBPIn, does not generate alkynylBPIn compounds under the reported conditions. Furthermore, this report does not invoke the intermediacy of Zn-C species or metathesis of Zn-C with H-B, potentially due to the current lack of precedence for such conversions. Therefore determining the feasibility of Zn-C / H-B metathesis is vital to establish the viability of borylation catalytic cycles mediated by molecular zinc hydrides. While molecular zinc hydrides have attracted significant attention in recent years, this is predominantly for the catalytic hydroboration of polar unsaturated bonds (e.g. C=O, C=N).¹⁴ In these systems C=O/C=N hydrozincation generates a zinc alkoxide or zinc amide which reacts with a hydroborane to regenerate the zinc-hydride and B-N or B-O containing products (Figure 1D). B-N and B-O bond formation provides a significant driving force (due to the partial multiple bond character present in B-N/B-O bonds) which will be absent in putative Zn-C / H-B metathesis reactions. It is however notable that Grignard reagents react with HBPIn to form Mg-H and organoBPIn species,¹⁵ thus suggesting the feasibility of an analogous metathesis reaction with organozinc compounds given the commonalities often observed between Mg and Zn chemistry.

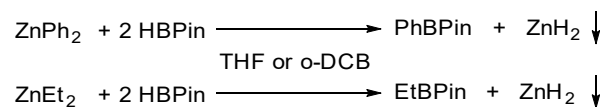
In this work we demonstrate that a range of organozinc species do undergo transmetalation with HBPIn to form organoBPIn species and zinc hydrides. The latter when ligated with bulky *N*-heterocyclic carbenes (NHC) are effective for both catalytic terminal alkyne C-H borylation and internal alkyne hydroboration. These two conversions can be combined using a single zinc catalyst to achieve the one-pot transformation of terminal alkynes into 1,1-diborated alkenes using HBPIn. 7-DIPP ligated Zn cations (inset Figure 1E, 7-DIPP = 1,3-bis(2,6-diisopropylphenyl)-4,5,6,7-tetrahydro-1H-1,3-diazepin-3-ium-2-ide) are essential for effective catalysis as this NHC affords enhanced thermal stability during catalysis (relative to zinc cations ligated by bulky five membered NHCs) and provides access to low coordinate zinc-hydride cations that are electrophilic yet Brønsted basic.

Results and Discussion

Zn-C / H-B Metathesis Studies

Commercial diphenylzinc was selected as the initial organozinc reagent for transmetalation studies as it is devoid of the equilibria present using organozinc-halides and it does not contain zincates which are often present when diorganozinc compounds

are made from Grignard reagents and ZnX₂. On mixing ZnPh₂ with two equiv. of HBPIn in THF rapid transmetalation proceeded leading to formation of PhBPIn as the major boron containing product (by ¹H and ¹¹B NMR spectroscopy). Insoluble material also was observed to form, presumably (ZnH₂)_∞. To confirm that THF coordination to any zinc species is not significantly affecting the transmetalation outcome the reaction was repeated in the more weakly coordinating solvent *ortho*-dichlorobenzene (*o*-DCB). From this reaction PhBPIn again was observed as the major boron product along with insoluble material (again presumably (ZnH₂)_∞). Similar outcomes were observed when combining commercial ZnEt₂ and HBPIn (with EtBPIn observed as the major boron containing product) confirming that Zn-C/H-BPin transmetalation proceeds with both dialkyl- and diaryl- zinc compounds.



Scheme 1: Zn-R / HBPIn transmetalation reactions.

Solubilizing the zinc hydride product formed post Zn-C/H-B transmetalation is essential to preclude precipitation shifting Zn-C/H-B metathesis equilibrium reactions to completion. Sterically demanding NHCs were selected as solubilizing ligands as low coordinate NHC-ligated zinc hydrides have been previously reported to be thermally stable at 20°C in solution for days while also being useful in a range of catalytic applications.¹⁴ The two NHCs selected were *N,N*-bis(2,6-diisopropylphenyl)-imidazol-2-ylidene (IDIPP) and 7-DIPP as these both have large percentage buried volumes (%V_{bur}) which enforces low coordination numbers at metal centres.¹⁶ (7-DIPP)ZnCl₂, **1**, and (7-DIPP)ZnPh₂, **2**, were synthesized by addition of the free carbene to ZnCl₂ and ZnPh₂, respectively. Notably, the solid state structures of both **1** and **2** on crystallization were monomeric and three coordinate at zinc. For the dihalide analogue **1** (which was crystallized from THF) this is in contrast to (IDIPP)ZnCl₂ which coordinated THF, forming (IDIPP)ZnCl₂(THF) which is four coordinate at Zn.¹⁷ Comparison of the buried volumes of **1** (49.7%) and **2** (44.7%) to a range of (IDIPP)Zn analogues confirms the greater steric impact of 7-DIPP relative to IDIPP. While the structure of **2** is comparable to previously reported (7-Mes)ZnMe₂,¹⁸ it is notable that there is a significant angle between the N-C-N plane and the PhC-Zn-C_{Ph} plane (64.6°) in **2** presumably reducing steric interactions between the DIPP and Ph moieties.

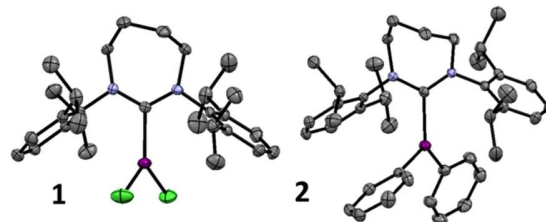
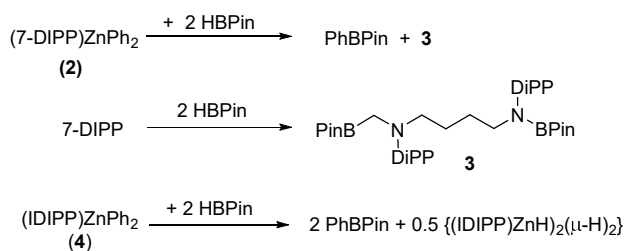


Figure 2. Solid state structures of **1** (left) and **2** (right) ellipsoids at 50 % probability and hydrogens omitted for clarity. Selected bond distances (Å) and angles (°) for **2**: NHC-C-Zn = 2.098(2); PhC-Zn = 1.989(2) and 2.011(2); PhC-Zn-C_{Ph} = 118.74(7); PhC-Zn-C_{NHC} = 123.75(7) and 116.90(7).

With a well-defined (NHC)ZnR₂ species in hand transmetalation with HBPIn was assessed. Compound **2** was combined with two equivalents of HBPIn in THF which led to the formation of PhBPIn as the major new boron containing product (by ¹H and ¹¹B NMR spectroscopy) along with other products, including the NHC-derived species, **3** (Scheme 2). In our hands a putative (7-DIPP)ZnH₂ complex could not be isolated from this mixture. Furthermore, other routes to form (7-DIPP)ZnH₂ species (commencing from **1** or **2**) were also unsuccessful in our hands. For full characterization the independent synthesis of **3** was achieved by combining 7-DIPP and 2 equiv. of HBPIn. Compound **3** is a NHC ring opened product derived from two H transfers from B to C and is related to previously reported products from the reaction of 1,3-bis(2,6-di-isopropylphenyl)-imidazolidin-2-ylidene (SIDIPP) with HBCat or HBPIn.¹⁹ The formation of **3** from reactions commencing from **2** / HBPIn would potentially also lead to (ZnH₂)_∞ formation, precipitation of which could still affect the metathesis equilibrium. To provide support for Zn-H formation by Zn-C/H-B metathesis being thermodynamically favored (IDIPP)ZnPh₂, **4**, was synthesized by the combination of IDIPP and ZnPh₂. Addition of two equivalents of HBPIn to **4** in *o*-DCB or THF led to formation of PhBPIn as the major new boron containing species along with the previously reported complex {(IDIPP)ZnH₂(μ-H)}₂.²⁰ This confirmed that in this case Zn-C/H-B metathesis is thermodynamically favored and not driven by the insolubility of one of the products.



Scheme 2: Top and bottom, transmetalation between (NHC)ZnPh₂ and HBPIn. Middle, the formation of **3**.

As zinc-catalyzed terminal alkyne C-H borylation (Scheme 1C) is the only zinc catalyzed C-H borylation reaction reported to date to the best of our knowledge,^{13a} we explored the transmetalation between Zn-alkynyl species and HBPIn. Zn-bis alkynyl complex **5** (Figure 3), was synthesized and crystallized from THF, with the solid-state structure indicating it is also three coordinate at zinc. Compound **5** has a shorter bond distance for NHC-C-Zn (2.037(3) Å) compared to **2** (2.098(2) Å) which contributes to the higher %V_{bur} determined for 7-DIPP in **5** (47.3°). There is also a large angle in **5** between the N-C-N and the alkynyl-C-Zn-C_{alkynyl} planes (89.2°) presumably to reduce steric interactions. The reaction of **5** with excess HBPIn in THF led to formation of alkynylBPIn **6a** and compound **3** (Figure 3, by ¹H and ¹¹B NMR spectroscopy after 18 h). Inspection of the *in-situ* NMR spectra at shorter reaction times revealed that the formation of NHC-ring opened product **3** occurs prior to formation of **6a**, indicating, in contrast to **2** and **4** that dissociation of 7-DIPP from zinc in compound **5** and formation of **3** occurs prior to the reaction of the resultant Zn(alkynyl)₂(THF)_n species reacting with HBPIn to form **6a**. Dissociation of bulky ring expanded NHCs from diorganozinc species has been previously

observed.¹⁸ Finally, for comparison the IDIPP congener, compound **7** (Figure 3 bottom), was synthesized *in-situ* from the reaction of **4** with two equiv. of 4-ethynyltoluene in THF (with evolution of benzene observed by NMR spectroscopy). This Zn-alkynyl species underwent transmetalation with excess HBPIn to form only one equivalent of **6a**, with the NHC remaining coordinated to zinc. The zinc containing product displayed NMR spectra consistent with the formulation {(IDIPP)Zn(alkynyl)(μ-H)}₂. With only one equivalent of HBPIn being consumed in the reaction with **7** (the second zinc-alkyne moiety does not undergo σ-bond metathesis even after long reaction times and with additional HBPIn added) this suggests that Zn-C_{alkynyl} / H-BPin metathesis is less energetically favorable than metathesis with Zn-Csp² analogues (e.g. **4**) where two metathesis steps take place.

Combined, the above reactions clearly demonstrate that Zn-C / H-B transmetalation between ZnR₂ / (NHC)ZnR₂ species and HBPIn proceeds for sp² and sp³ carbon centres and to some extent for C-sp centres. With the viability of metathesis confirmed and the reactivity of molecular zinc hydrides with terminal alkynes to form zinc alkynyls and H₂ previously documented²¹ the feasibility of combining these steps to achieve zinc catalyzed alkyne borylation with HBPIn was explored.

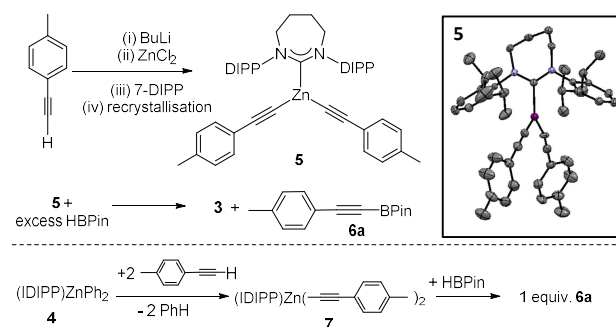
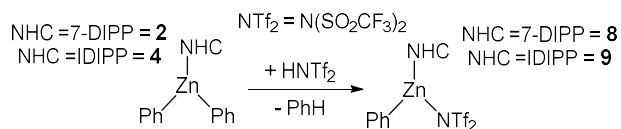


Figure 3. Top, the synthesis of **5** and inset its solid state structure (ellipsoids at 50% probability and hydrogen atoms omitted for clarity). Middle, transmetalation between **5** and HBPIn. Bottom, transmetalation between compound **7** (formed *in-situ*) and HBPIn. Selected bond distances (Å) and angles for **5** (°): NHC-C-Zn = 2.037(3); alkynyl-C-Zn = 1.969(4) and 1.959(4); alkynyl-C-Zn-C_{alkynyl} = 115.75(14); alkynyl-C-Zn-C_{NHC} = 119.61(13) and 124.59(13).

Catalytic Terminal Alkyne C-H Borylation

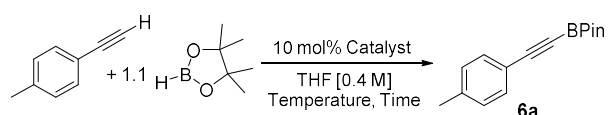
Catalytic studies started with compounds **2** and **4** as these are readily accessible catalyst precursors with the proposed on-cycle (NHC)Zn-hydride species generated by transmetalation with HBPIn (forming PhBPIn as the by-product). However, using **2** or **4** as the (pre)catalyst in *o*-DCB, MeCN or THF under a range of conditions led to only partial consumption of 4-ethynyltoluene, incomplete (< 50% in all cases) formation of the desired compound **6a** and formation of multiple other products (by *in-situ* multinuclear NMR spectroscopy) some of which were consistent with products from the reaction of the NHC with HBPIn (e.g. **3**). During these reactions using **2** or **4** insoluble material also was observed to form concomitant with catalyst deactivation. Catalyst decomposition (as indicated by precipitation of insoluble material) occurred more readily on heating to 60°C with no significant improvement in the conversion to **6a** using **2** or **4**.



Scheme 3: Protonolysis of **2** and **4** to form complexes **8** and **9**.

With catalyst deactivation potentially precluding high conversions to **6a** using **2** or **4** cationic analogues of general formula (NHC)ZnPh(anion) were targeted, as hydrides of the general formula, (NHC)Zn(H)(anion), have been reported to be significantly more thermally stable than neutral (NHC)ZnH₂ analogues.^{14c} Compound **2** was combined with one equivalent of the strong Brønsted acid HNTf₂ which led to benzene evolution and formation of (7-DIPP)ZnPh(NTf₂), **8**. (IDIPP)ZnPh(NTf₂), **9**, was synthesized via an analogous route (Scheme 3).

Table 1. Catalyst optimization for alkyne dehydroboration



Entry	Catalyst	T (°C)	Time / h	6a ^d
1	8	20	72	94
2	8	40	18	89
3	8	60	2.5	85
4	8^a	60	5	99
5	9^a	60	1.5	7
6	9^a	60	21	11
7	ZnPh ₂	60	5	2
8	PhZnNTf ₂ ^b	60	5	5
9 ^c	8 + base	20	18	41

Reaction conditions as shown above unless otherwise indicated. a = using 5 mol% at [0.8 M] **8** b = made *in-situ* from ZnPh₂ / HNTf₂. c = base = 2,4,6-tri-*tert*-butylpyridine. d = Yields by *in-situ* ¹H NMR spectroscopy based on the ratio of the product Vs. mesitylene added as internal standard.

In *o*-DCB or benzene the use of **8** as a borylation catalyst did proceed but led to competitive terminal alkyne C-H borylation and hydroboration in *o*-DCB (approx. 1 : 1 mixtures of products were formed) while in benzene the C-H borylation product dominated but lower yields were observed (ca. 75%). In contrast, in THF only alkyne C-H borylation to form **6a** was observed over a range of reaction temperatures. While alkyne C-H borylation in THF was slow at 20°C reactions with **8** could be heated in THF (table 1, entries 1-4) without significant catalyst deactivation, thus enabling high conversion to **6a**. Notably, under a range of conditions the (IDIPP)Zn analogue **9** gave very low conversions (e.g. entries 5 and 6). Reactions using **9** led to the formation of a black precipitate on heating at 60°C, consistent with the formation of zinc metal and indicating the lower thermal stability under these catalytic conditions for (IDIPP)Zn congeners versus (7-DIPP)Zn congeners. This is consistent with the absence of any additional turnover with longer reaction times (entries 5 Vs 6). In the absence of any NHC, using ZnPh₂ or PhZnNTf₂ as catalysts, extremely low conversions were observed (entries 7-8) indicating the importance of NHC ligation.

Finally, in an attempt to use a base to catalyze any alkyne deprotonation steps (as proposed previously for zinc catalyzed alkyne C-H borylation with HBDan, see Figure 1C)^{13a} compound **8** was utilized in combination with a hindered pyridyl base (to prevent pyridyl coordination to zinc and catalyst deactivation as observed previously in carbonyl hydrosilylation using related zinc systems)^{14e}. However, this resulted in no significant increase in conversion (entry 9) relative to borylation reactions in the absence of this base, indicating under these conditions that this base is not involved in any deprotonation step.

With effective zinc catalyzed alkyne C-H borylation conditions in hand, the borylation of a range of terminal alkynes was investigated. Aryl, heteroaryl, vinyl and alkyl substituted alkynes were all viable substrates with 1.1 equiv. of HBpin sufficient for high yields of **6** in each case (Figure 4). This methodology was also applicable to a range of terminal arylalkynes bearing electron donating and withdrawing functionalities such as OMe, F, Cl, NMe₂ and CF₃. However, substrates containing nitrile and nitro-substituents were not amenable as these were reduced in preference to alkyne C-H borylation. Given the large steric demand of 7-DIPP it is notable that *ortho*-ClC₆H₄ and mesityl substituted alkynes, **6g** and **6i**, were successfully borylated under these conditions.

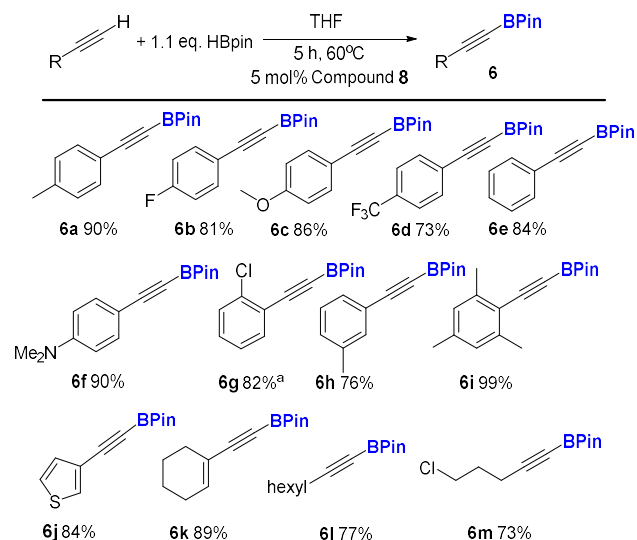


Figure 4: Scope of (7-DIPP)Zn catalyzed alkyne C-H borylation. Yields by *in-situ* ¹H NMR spectroscopy based on the ratio of product Vs. mesitylene added as internal standard. a = 22 h.

Formation of 1,1-Diborylated Alkenes

While alkynyl boronate esters such as **6a-m** are useful in their own right²² they are highly prone to protodeborylation. Therefore we sought to perform a subsequent transformation of the alkynyl boronate esters *in-situ* using the same zinc catalyst targeting more robust to protodeborylation products that are also highly useful. Guided by the observation of alkyne hydroboration as a by-product during the formation of **6a** in aromatic solvents we targeted the hydroboration of **6a**. This reaction would proceed via initial alkyne hydrozincation with a subsequent transmetalation of the Zn-alkenyl intermediate with HBPin furnishing diborylated alkenes (e.g. **10a**, Figure 5). Notably, while Zn-B and Zn-Si bonds have been reported to add to alkynes in

the absence of catalysts,²³ to the best of our knowledge, catalyst free alkyne hydrozincation has not been reported prior to this work.²⁴ The hydroboration of alkynyl boronate esters could produce 1,1 or 1,2 diborylated alkenes, both useful products.^{8,25} However, catalytic routes to form the 1,1-isomer from non-activated alkynes (e.g. alkynes that are not Michael acceptors)²⁶ are much more limited with those reported to date requiring noble metal or cobalt catalysts.⁷

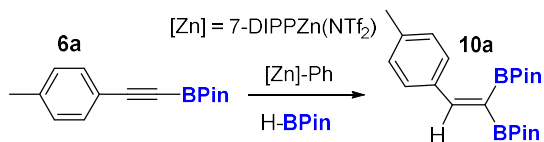


Figure 5: Hydroboration of **6a** to **10a** using precatalyst **8**.

The hydroboration of **6a** using HBPIn and 10 mol% **8** as a catalyst precursor was achieved in good yield on heating in a range of hydrocarbon solvents (toluene, benzene or methyl-cyclohexane). In hydrocarbon solvents the 1,1-diborylated alkene, **10a**, was formed in high yield (> 95% after heating for 28 h at 90°C) with no 1,2-isomer observed by NMR spectroscopy. To provide support that the catalysis is zinc mediated and that B-H species formed by borane substituent redistribution (minor ¹¹B resonances centered at 22 ppm are observed during this process consistent with formation of (RO)₃B products) are not responsible for the observed hydroboration of **6a**,²⁷ control experiments using BH₃.THF were carried out. Using 10 mol% BH₃.THF (1M in THF) only 25% hydroboration of **6a** to **10a** was observed after 33 hours at 90°C. This is drastically less than the outcome observed using 10 mol% of **8** as a precatalyst which gives complete conversion of **6a** to **10a** under identical conditions. Hydroboration conversion using **8** remains high (> 98% conversion after 28 h) even when 5 equivalents of THF was added to the reaction mixture (disfavoring THF being a catalyst poison). These results suggest that (7-DIPP)Zn based species are responsible for the hydroboration reactivity, which proceeds via a highly selective hydrozincation of **6a** and subsequent transmetalation with HBPIn.

A combined C-H borylation / hydroboration protocol next was developed to form 1,1-diborylated alkenes in one-pot from terminal alkynes operating all in hydrocarbon solvent (C₆D₆ is used in sealed tubes for NMR monitoring purposes but the transformation also proceeds effectively in toluene). The one-pot conversion of the terminal alkyne to **10a** using **8** as the catalyst precursor proceeded in good yield at 90°C with no solvent switch required. Notably, performing the reaction in C₆D₆ at the lower temperature of 60°C led to **6a** being the major product with minimal formation of **10a** observed. The higher temperature required to form **10a** indicates a greater kinetic barrier (relative to formation of **6a**) and that C-H borylation precedes hydroboration under these conditions. With conditions in hand using **8** as a catalyst precursor a number of terminal alkynes were converted in one-pot to the 1,1-diborylated alkenes, **10a-h**, in moderate to good yield without isolation of the intermediate alkynyl boronate esters **6** (Figure 6). Performing the tandem functionalization for longer duration or increasing the number of equivalents of HBPIn used (from 4 to 5) increases the conversion to the 1,1-diborylated alkenes, indicating that there is still significant catalyst remaining (the mass balance in these reactions is predominantly **6x**). This one-pot diborylation process was amenable to a range of terminal alkynes (including aryl groups substituted with electron withdrawing and donating groups and *ortho*, *meta* and *para* substituents). It should be

noted that electron withdrawing groups required longer for comparable conversion, suggesting a build-up of cationic character on the alkyne moiety in the transition state of the hydrozincation process. This transformation complements the recently reported cobalt catalyzed conversion of terminal alkynes into 1,1-diborylated alkenes (which focused predominantly on alkyl alkynes). Furthermore, this zinc catalyzed process proceeds with no enyne by-products from homodimerization observed in contrast to the cobalt catalyzed process.^{7b} As the diborylated alkene products, **10**, are much more resistant to protodeborylation than the respective alkynyl boronate esters they are readily isolated by column chromatography in moderate to good yields. 1,1-diborylated alkenes have been previously utilized in a wide range of transformations (e.g. Suzuki-Miyaura cross coupling, halogenation to the 1,1-dihaloalkenes and oxidation to carboxylic acids) thus are extremely useful.^{7,8}

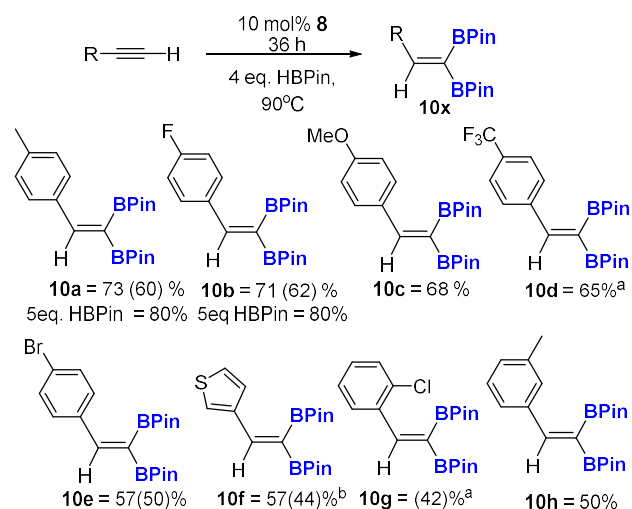


Figure 6: The conversion of terminal alkynes into 1,1-diborylated alkenes in C₆D₆ using precatalyst **8**. Yields are by NMR spectroscopy based on the ratio of the product formed versus an internal standard (isolated yields are provided in parentheses). a = reaction run for 56 h, b = 48 h.

Mechanistic Studies

Precatalyst Activation and Synthesis of Zn-H Species:

Compound **8** is a readily accessed catalyst precursor, with a plausible mechanism (Figure 7) commencing by **8** undergoing transmetalation with HBPIn to form a low coordinate [(7-DIPP)ZnH]⁺ species (presumably solvent and/or anion coordinated). Alternatively, **8** can react with a terminal alkyne by protonolysis to evolve benzene and form [(7-DIPP)Zn(alkynyl)]⁺ species (again the zinc centre will be solvent / anion coordinated). These two cations represent the key proposed on-cycles species that would enable the first process, terminal alkyne C-H borylation. Inspection of the catalytic C-H borylation reactions (in THF and in benzene) by *in-situ* ¹H and ¹¹B NMR spectroscopy indicated the presence of PhBPIn in all cases formed by Zn-Ph/H-BPin metathesis. In contrast, no formation of benzene (the expected by-product from protonolysis of **8** with the terminal alkyne) was observed in THF under these conditions by ¹H and ¹³C{¹H} NMR spectroscopy. This confirms that Zn-Ph / H-B transmetalation is kinetically more facile under these conditions than Zn-Ph protonolysis and thus metathesis is the key step for accessing zinc-hydride species in this system.

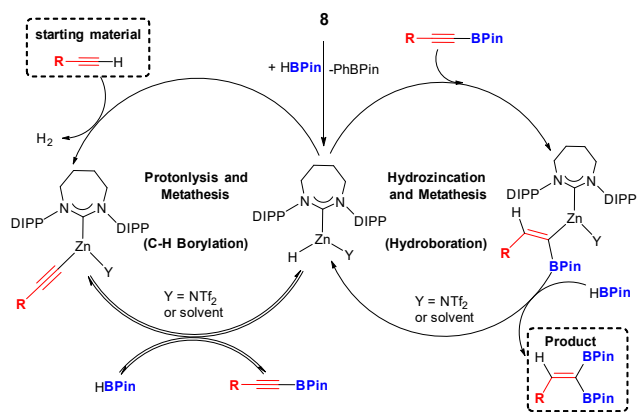


Figure 7: Proposed mechanism for terminal alkyne diboration.

Isolation and structural characterization of the various (7-DIPP)Zn complexes shown in Figure 7, particularly the proposed zinc hydride was targeted. Compound **8**, (7-DIPP)ZnPh(NTf₂), was isolated as a crystalline solid from THF with the [NTf₂]⁻ anion bound to the zinc center in a bidentate fashion (Figure 8, left) with no THF bound to zinc in the solid state structure. The majority of the structural metrics for **8** are comparable to the related four coordinate complex (NHC)Zn(C₆F₅)(O₂CR), **A** (where the carboxylate is also bidentate, R = Cp*),²⁸ with similar C-Zn distances. However, the Zn-O distances in **8** (in the range 2.314(2) to 2.236(2) Å) are much larger than that in **A** (Zn-O = 2.086(2) Å)²⁸ suggesting that [NTf₂]⁻ in **8** is more weakly interacting with the zinc centre.

To confirm that Zn-C/H-B transmetalation does proceed from **8**, **8** was reacted with HBPIn in THF at 60°C. Transmetalation between **8**/HBPIn in THF does form PhBPIn, however, in the absence of terminal alkyne (to react with the zinc-hydride product) subsequent reaction with more HBPIn occurs in THF to form **3** and other currently unidentified products, preventing isolation of a zinc-hydride. However, in *o*-DCB the transmetalation between **8**/HBPIn proceeds cleanly and alongside PhBPIn a single new zinc product that contained a resonance consistent with a terminal Zn-H (δ_{1H} = 3.65 ppm 1 H integral relative to the new NHC resonances) was observed as the major new (7-DIPP)Zn species. This species was isolated by recrystallization with its solid state structure confirming its formulation as (7-DIPP)ZnH(NTf₂), **11**, with NTf₂ again bound to zinc in a bidentate manner (Figure 8 middle). The structural metrics of **11** are closely comparable to **8** (with **11** also having relatively long Zn-O distances 2.232(2) and 2.252(2) Å), again suggesting that NTf₂ is weakly coordinating to zinc. Comparison of **11** with the related complex (IDIPP)Zn(H)(N(SiMe₃)₂)²⁹ **B**, reveals a comparable δ_{1H} for the Zn-H (3.20 ppm for **B**). While many structural metrics are comparable between **B** and **11**, the C-Zn-H angle in **11** is considerably greater than observed in **B** (149(3) for **11** and 107.9(1)° for **B**), consistent with a weaker interaction between zinc and NTf₂ in **11** than between zinc and N(SiMe₃)₂ in **B**, with **11** approaching the geometry observed in two coordinate [(NHC)Zn-R]⁺ complexes (R = Et or C₆F₅) which have C-Zn-C angles approaching 180 (173 and 175).^{14g}

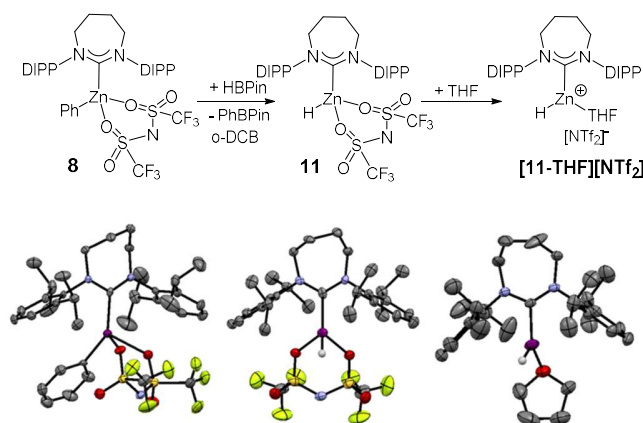


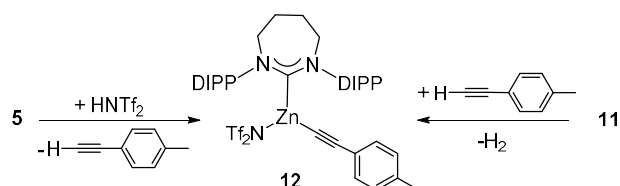
Figure 8: Synthesis of **11** from **8** in *o*-DCB and subsequent NTf₂ dissociation observed on recrystallization from THF. Bottom, solid state structures of **8**, **11** and [11-THF]⁺, ellipsoids at 50% probability and most hydrogens omitted for clarity. Selected bond distances (Å) and angles (°) for **8** C_{NHC}-Zn = 2.050(3), C_{Ph}-Zn = 1.992(2), C-Zn-O = 2.293(2) and 2.236(2), C_{NHC}-Zn-O = 105.39(9) and 114.46(9) C-Zn-C = 141.7(1). For **11** C-Zn = 2.035(5), Zn-O = 2.233(2) and 2.252(2), 1.39(8), C-Zn-O = 112.9(2) and 109.2(2) Zn-H = 1.39(8). For [11-THF]⁺ Zn-C = 2.006(4), Zn-H = 1.48(6), Zn-O = 2.108(4), C-Zn-O = 112.1(1).

With alkyne C-H borylation catalysis optimal in THF determining the speciation of **11** in THF is important. Increasing equivalents of THF were added stepwise to **11** dissolved in *d*₅-bromobenzene which resulted in a gradual upfield shift of the Zn-H resonance (the Zn-H moiety in **11** resonates at 3.65 ppm in *d*₅-bromobenzene, but at 3.22 ppm in *d*₈-THF). Confirmation of THF coordination to zinc was forthcoming from the solid state structural analysis of crystals obtained from a THF solution of **11**. This revealed displacement of NTf₂ by one molecule of THF and formation of a three coordinate Zn-H cation, [(7-DIPP)Zn(H)(THF)]⁺, termed [11-THF]⁺. The closest anion---zinc contacts are all long, with 5.41 Å the shortest Zn---F and 5.93 Å the shortest Zn---O contact to NTf₂. The geometry at zinc in [11-THF]⁺ is approximately trigonal planar (Σ (angles) at Zn = 359.2°) with a relatively (compared to **B**) large C-Zn-H angle again observed (133(2)). Other bulky NHCs coordinated to cationic zinc-hydrides lead to \geq four coordinate zinc centres due to solvent/anion coordination or oligomerization.¹⁴ While 2 and 3-coordinate neutral zinc hydride complexes are known,³⁰ [11-THF]⁺ is the first example of a low (< 4) coordinate cationic zinc hydride, to the best of our knowledge, which is accessible due to the large steric demand of the 7-DIPP ligand.

Alkyne C-H-Borylation:

The solution state reactivity of **11** relevant to the catalytic cycle proposed in Figure 7 next was explored. Firstly, using **11** in place of **8** as catalyst in the C-H borylation to form **6a** resulted in a greater conversion to **6a** after 90 minutes relative to the conversion when using **8**. Furthermore, no induction period is observed for the formation of **6a** when using **11**. This is consistent with **11** (or [11-THF]⁺) being an on-cycle species, or having a low barrier to form an on-cycle species. Next, **11** was reacted with 4-ethynyl toluene, which led to concomitant consumption of both the Zn-H and alkynyl C=C-H resonances in

the ^1H NMR spectrum and the formation of a single major (7-DIPP)Zn containing product. This new species was not isolable in our hands, however, the same compound was obtained by reaction of **5** with one equivalent of HNTf_2 (by ^1H NMR spectroscopy), with the expected terminal alkyne by-product from protonolysis observed (Scheme 4). This supports the identification of this new complex as $[(7\text{-DIPP})\text{Zn}(\text{alkynyl})\text{NTf}_2]$, **12**, which again maybe anion and/or solvent coordinated.



Scheme 4: Formation of compound **12** (shown as anion coordinated, in THF solution THF could also be bound to zinc, displacing NTf_2 to produce $[\text{12-THF}]^+$).

The use of **12** in the C-H borylation catalysis in THF also led to effective formation of **6a** with a greater conversion after 90 minutes relative to that using **8**, indicating **12** is also an on-cycle species, or has a low barrier to form an on-cycle species. The addition of HBPIn to **12** (in the presence of one equiv. of 4-ethynyl toluene) resulted in formation of **6a** (the zinc-hydride, **11** or $[\text{11-THF}]^+$, is not observed by NMR spectroscopy as it is consumed by the rapid reaction with 4-ethynyl toluene to reform **12**) confirming the feasibility of this Zn-alkynyl / H-BPin metathesis step. Repeating the reaction between **12** and excess HBPIn in THF in the absence of any additional terminal alkyne still led to formation of **6a**, but the ring opened NHC derived product **3** was observed instead of the zinc-hydride (**11** or $[\text{11-THF}]^+$), consistent with **11** not being stable in THF in the presence of excess HBPIn. Thus, all the steps of the proposed C-H borylation cycle shown in Figure 7 are viable, but in THF the zinc hydride **11** can react with additional HBPIn (leading to catalyst deactivation) or with a terminal alkyne (leading to turnover), with the latter reaction dominating. Notably, the combination of stoichiometric **11** and **6a** in C_6D_6 (a solvent in which combinations of **11**/HBPIn do not result in decomposition to form **3**) leads to formation of HBPIn as the major boron containing species (Figure 9) and resonances consistent with **12**. However, not all **11** and **6a** are consumed (even on heating) in this reaction. These observations suggest that formation of zinc hydride **11** and **6a** from **12** and HBPIn is an equilibrium process favouring **12** and HBPIn and that consumption of **11** in a subsequent step (e.g. reaction with a terminal alkyne to form H_2 and reform **12**) is required to drive the reaction to completion.

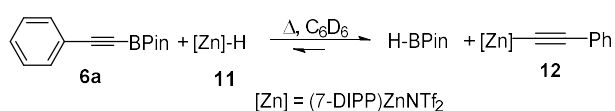


Figure 9: Reversible sigma bond metathesis between zinc alkynyl **12** and HBPIn.

Alkyne Hydroboration:

Regarding the second cycle in figure 7, the alkynyl boronate esters are proposed to undergo hydrozincation and then metathesis with HBPIn to form the diborylated alkenes. Hydroboration of **6a** is more effective in hydrocarbon solvents than in THF, an

observation attributable to the decomposition of zinc-hydride **11** in the presence of excess HBPIn in THF (and in the absence of terminal alkyne). In contrast, in benzene and other weakly coordinating solvents (e.g. *o*-DCB) **11** is more robust towards decomposition from reaction with HBPIn, permitting prolonged heating which is essential for the transformation of **6** into **10**. To the best of our knowledge uncatalyzed hydrozincation of alkynes has not been previously documented. However, direct observation of hydrozincation products by combining **11** and **6a** is complicated by the kinetic product being the zinc-alkynyl **12** and HBPIn. It is only on prolonged heating that the diborylated products **10** are observed, indicating they are the thermodynamic products from this reaction and suggesting that the hydrozincation of **6a** with **11** has a higher barrier than the σ -bond metathesis to form **12** and HBPIn.

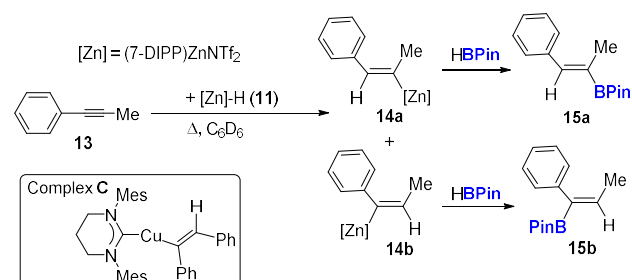


Figure 10: Hydrozincation of alkyne **13** with **11** and subsequent metathesis with HBPIn. Inset, complex **C**.

To probe the feasibility of the unprecedented catalyst free alkyne hydrozincation step the internal alkyne 1-phenyl-1-propyne, **13**, was reacted with stoichiometric **11** in C_6D_6 . While no reaction was observed at room temperature, on heating complete consumption of both **11** and **13** was observed, producing two new species in an approximately 1:1 ratio. These were spectroscopically consistent with the hydrozincation products **14a** and **14b** (Figure 10). Key diagnostic resonances from the ^1H NMR spectrum included a new alkenyl singlet at 5.32 ppm (for **14a**) and a quartet at 4.82 ppm (for **14b**), the latter is coupled to the alkenyl-Me group. In the HSQC spectrum these resonances were found to correlate to $\delta_{13\text{C}}$ alkenyl resonances at 142.6 and 140.3 ppm. Crucially, both of these species undergo σ -bond metathesis with HBPIn to afford the previously reported vinylboronate esters **15a** and **15b**.³¹ Surprisingly, no well-defined zinc alkenyl complexes are reported in the literature, to the best of our knowledge, but support for the observed alkenyl chemical shifts for **14a** and **14b** is forthcoming from complex **C** (inset Figure 10) which has an alkenyl C-H resonance at 5.65 ppm (in contrast alkenylBPIn C-H resonates significantly further downfield).³¹ The selectivity in the hydrozincation/hydroboration of **13** is low in contrast to that observed in the hydroboration of **6**. We attribute this disparity to the cationic nature of the zinc centre in **11**, leading to build-up of positive charge on the alkyne during hydrozincation which is significantly more stabilized by the aryl moiety than the BPin in **6** leading to the observed selective formation of 1,1-diborylated products. In contrast with alkyne **13** the electronic disparity between Ph / Me is less (than Ph/BPin) resulting in lower selectivity.

DFT Calculations

Catalyst Speciation / Key Properties

The mechanistic studies discussed above indicate the involvement of zinc-hydride and zinc-alkynyl complexes in alkyne C-H borylation, with both potentially being three coordinate mono solvated (NHC)Zn cations in THF. To determine the degree of solvation in THF for subsequent computational investigations the energy change on binding of a second molecule of THF to $[\mathbf{11-THF}]^+$ was explored at the M06-2x/cc-pVTZ level. This was performed as regardless of the solid state structure in solution it is feasible that an additional THF molecule binds to zinc in $[\mathbf{11-THF}]^+$. At this level the calculated structure of $[\mathbf{11-THF}]^+$ revealed similar metrics to the solid state structure. For $[\mathbf{11-THF}]^+$ the binding of a second molecule of THF to zinc was found to be effectively thermoneutral at 298 K (Figure 11), therefore the three coordinate at zinc species, $[\mathbf{11-THF}]^+$, will dominate at raised temperatures and thus mono-solvated species are used in all the subsequent DFT calculations (including the hydrosilycation process).³²

Analysis of the electronic structure of $[\mathbf{11-THF}]^+$ revealed that despite the low coordination number at zinc and the unit positive charge the hydride has significant negative charge (-0.544) based on natural bond orbital (NBO) calculations. This is comparable in magnitude to that previously calculated (at the same level) for the hydride in the four coordinate (at zinc) complex (IDIPP)ZnH(THF)(OTf).^{14c} Another notable point is that the LUMO of $[\mathbf{11-THF}]^+$ has significant zinc p orbital contribution, in contrast to the four coordinate at zinc bis-solvate complex $[\mathbf{11-THF}_2]^+$ (Figure 11, inset) which has negligible zinc contribution to the LUMO. Finally, the energy of the LUMO of $[\mathbf{11-THF}]^+$ is significantly lower than for $[\mathbf{11-THF}_2]^+$ as expected based on their respective coordination numbers. Thus $[\mathbf{11-THF}]^+$ contains a highly electrophilic zinc centre and an hydridic (thus Brønsted basic) Zn-H moiety.

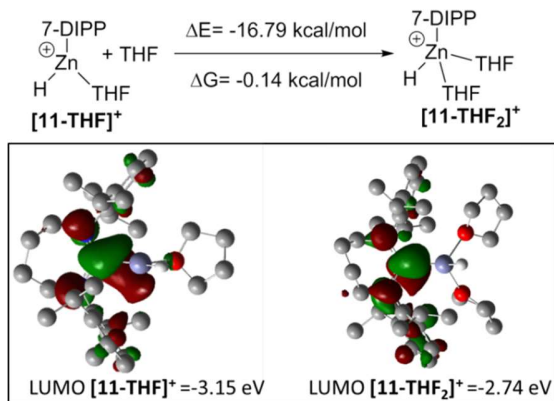


Figure 11: Top, energy change on binding a molecule of THF to $[\mathbf{11-THF}]^+$. Inset left, LUMO of $[\mathbf{11-THF}]^+$ and inset right LUMO of $[\mathbf{11-THF}_2]^+$ (iso surface value = 0.04, hydrogens omitted for clarity apart from Zn-H). NBO charges for $[\mathbf{11-THF}]^+$: $C_{NHC} = +0.090$, $Zn = +1.155$, $Zn-H = -0.544$, $O = -0.661$.

C-H Borylation:

Regarding the feasibility of the proposed C-H borylation mechanism outlined in Figure 7, the σ bond metathesis step was explored at the M06-2X/cc-pVTZ level and at the computationally less demanding M06-2x/lanl2dz/6-311g/PCM(THF) level. At both these levels the calculated ΔG values were all within 2

kcalmol⁻¹, thus further calculations were performed at the M06-2x/lanl2dz/6-311g/PCM(THF) level, and only values at this level are reported from here on unless otherwise stated. Starting from the zinc-alkynyl species $[\mathbf{12'-THF}]^+$ ($\mathbf{12'}$ designates it contains a phenylacetylene unit not 4-ethynyltoluene), the transmetalation with HBPIn to form $[\mathbf{11-THF}]^+$ is endergonic, but only by +4.1 kcalmol⁻¹ (Figure 12). The subsequent protonolysis of $[\mathbf{11-THF}]^+$ is exergonic, with the formation of H₂ presumably playing a key role in the overall favorable energetics of the conversion due to the high bond energy of H₂. The overall conversion of phenylacetylene / HBPIn to H₂ and $\mathbf{6e}$ is exergonic by 6.1 kcalmol⁻¹. The transition state (TS1) for the key σ -bond metathesis step from the spectroscopically observed resting state (the zinc-alkynyl, $[\mathbf{12'-THF}]^+$) to the zinc-hydride $[\mathbf{11-THF}]^+$ was relatively low in energy, $\Delta G^\ddagger = +19.3$ kcal mol⁻¹ (relative to $[\mathbf{12'-THF}]^+$ / HBPIn). These results are consistent with the observed reactivity, with the presence of additional terminal alkyne required to react with the hydride $[\mathbf{11-THF}]^+$ whose formation is slightly endergonic from $[\mathbf{12'-THF}]^+$ and HBPIn.

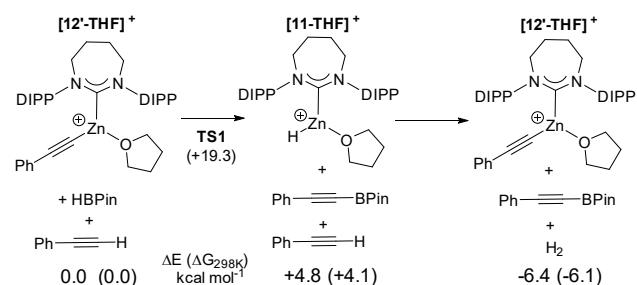


Figure 12: Calculations at the M06-2x/lanl2dz/6-311g/PCM(THF) level for: top, the C-H borylation process.

In contrast to the reactivity of the (7-DIPP)Zn-alkynyl complex $\mathbf{12}$ with HBPIn (an endergonic reaction), the reaction of the phenyl derivative, $\mathbf{8}$, with HBPIn furnishes the zinc-hydride complex $\mathbf{11}$, indicating an exergonic reaction. Examining this transformation confirmed the transmetalation of $[\mathbf{8-THF}]^+$ with HBPIn to form $[\mathbf{11-THF}]^+$ and PhBPIn is exergonic (by 9.0 kcalmol⁻¹, Figure 13). Inspection of the electronic structure of $[\mathbf{8-THF}]^+$ and $[\mathbf{12'-THF}]^+$ for any significant differences reveals closely comparable LUMOs (for the LUMO of $[\mathbf{8-THF}]^+$ see Figure 13), but distinct occupied frontier orbitals. For $[\mathbf{8-THF}]^+$, the HOMO has significant Zn-C sigma bond character; however, for the alkynyl analogue, $[\mathbf{12'-THF}]^+$, the HOMO has PhC≡C π character. It is the lower in energy HOMO-8 of $[\mathbf{12'-THF}]^+$ that is the highest energy occupied orbital that contains significant Zn-C sigma bond character, which indicates a reduced nucleophilicity of the zinc-alkynyl moiety relative to the zinc-phenyl. Regarding the thermodynamics of σ -bond metatheses, recent work has determined that the bond dissociation energy for the C-B bond in alkynyl-boronic acids is significantly (*ca.* 25 kcal mol⁻¹) greater than the C-B bonds in phenyl boronic acids.³³ This indicates that the zinc-alkynyl bond in (7-DIPP)-Zn compounds has to be significantly stronger than the Zn-Ph bond for the reaction of zinc-hydride $\mathbf{11}$ and $\mathbf{6a}$ to form HBPIn / $\mathbf{12}$ to be thermodynamically favored. This difference is further supported by the isodesmic reaction (bottom inset, Figure 13) between PhBPIn/ $[\mathbf{12'-THF}]^+$ and $\mathbf{6e}$ / $[\mathbf{8-THF}]^+$ which is found to be significantly exergonic. We attribute this to the greater C 2s orbital character in the Zn-C(alkynyl) bond relative to that in the

Zn-C_(Ph) bond. This will lead to a greater degree of δ^+ Zn-C δ^- polarization for the alkynyl derivative and thus a greater electrostatic contribution enhancing the Zn-C bond strength relative to the phenyl derivative as discussed previously for other series of organometallic complexes.³⁴ Due to the difference in the respective valence orbital energies of Zn and B this effect will be greater for organozinc species than organoboron species. Consistent with this hypothesis is the observation that the magnitude of positive charge on zinc is greater in the alkynyl derivative **[12[']-THF]**⁺ relative to the phenyl derivative **[8-THF]**⁺ (+1.391 compared to +1.366) based on NBO calculations.

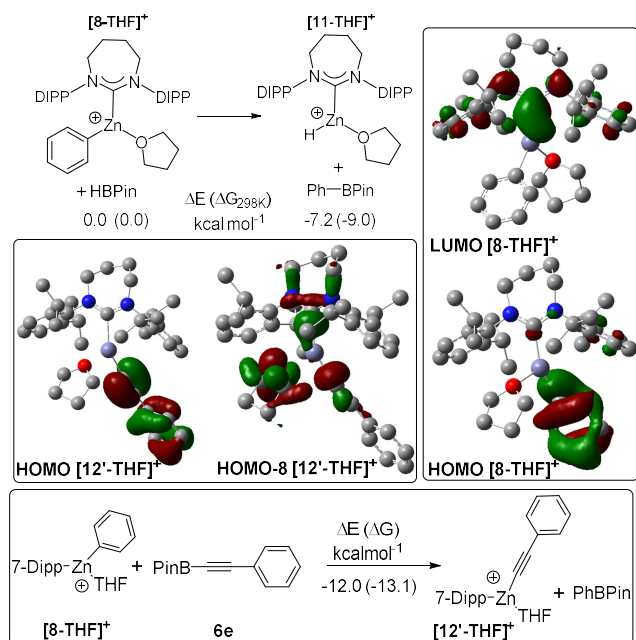


Figure 13: The exergonic metathesis of **[8-THF]**⁺ and HBPIn. Inset, key select frontier orbitals of **[12[']-THF]** and **[8-THF]**⁺ (iso surface value = 0.04). Bottom, the isodesmic reaction between Zn-C/B-C species.

Alkyne Hydrozincation:

The energetic feasibility of internal alkyne hydrozincation was next explored. The fact that hydroboration is not observed in THF or in benzene at lower temperatures ($\leq 60^\circ\text{C}$) suggested a significant barrier (as the Zn-C/H-B metathesis steps explored in this work have all been found to be facile). Hydrozincation calculations utilized the internal alkyne **13**, where the Zn-alkenyl products, **14**, are observed spectroscopically. Calculations indicated that while the hydrozincation of alkyne **13** using **[11-THF]**⁺ was significantly exergonic the transition states (**TS2** and **TS3**, Figure 14) were found to be relatively high in energy (compared to **TS1**) in both cases. These barriers are consistent with the requirement for heating for internal alkyne hydrozincation/hydroboration to occur. The highly exergonic nature of alkyne hydrozincation indicates it will proceed irreversibly, consistent with it being the thermodynamic pathway. Inspection of **TS2** (**TS3** is extremely similar in character) reveals a considerable deviation from linearity of the alkyne moiety (C-C≡C angles are 143° and 153°), elongation of the C≡C bond (to 1.25 Å) and the Zn-H bond (from 1.65 Å in **[11-THF]**⁺ to 1.74 Å in **TS2**) and contraction of the C-H distance (to 1.79 Å). Thus these calculations support the feasibility of the mechanism proposed in figure 7.

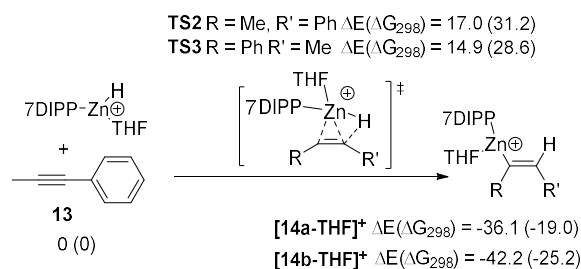


Figure 14: The calculated transition state and product energies (in kcal mol⁻¹) for the hydrozincation of **13** with **[11-THF]**⁺.

NHC Dependency:

Finally, the dramatic disparity in catalytic performance observed between 7-DIPP and IDIPP was investigated. One major difference between the two series of (NHC)Zn complexes is the relative accessibility of the respective three coordinate zinc complexes. The binding of a second molecule of THF to **[(IDIPP)Zn(H)THF]**⁺, **[16-THF]**⁺, to form **[16-THF₂]**⁺ (Figure 15, top) is exergonic by 7.6 kcal mol⁻¹ (calculated at the M06-2x/cc-pVTZ level for comparison with the 7-DIPP analogue see Figure 11). The exergonic nature of this step is in contrast to the energetically neutral nature of THF binding for the 7-DIPP analogue **[11-THF]**⁺. As observed for **[11-THF₂]**⁺ binding of two THF molecules to zinc increases the energy and alters the character of the LUMO which in both **[11-THF₂]**⁺ (Figure 11, bottom) and **[16-THF₂]**⁺ (Figure 15, bottom) is higher in energy and has no significant character on zinc in contrast to the three coordinate mono-THF congeners **[11-THF]**⁺ and **[16-THF]**⁺ (the LUMO for **[16-THF]**⁺ is closely comparable to that calculated for **[11-THF]**⁺, see figure 11).

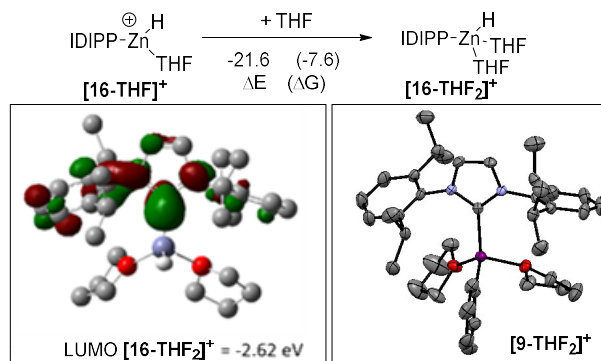


Figure 15: Top, exergonic binding of a second molecule of THF at 298 K (in kcal mol⁻¹) to **[16-THF]**⁺. Inset left, LUMO of **[(IDIPP)ZnH(THF)₂]**⁺ (**[16-THF₂]**⁺) at isosurface value = 0.04 (most hydrogens omitted for clarity), inset right solid state structure of **[9-THF₂]**⁺, select bond distances (Å) = Zn-C_{Ph} = 1.982(3), Zn-C_{NHC} = 2.044(3), Zn-O = 2.134(2) and 2.044(2).

To confirm that **(IDIPP)Zn(NTf₂)Y** (Y = H, Ph or alkynyl) complexes can indeed coordinate two molecules of THF we attempted to crystallize a number of **(IDIPP)Zn(NTf₂)Y** complexes from THF. Crystals of **9** formed from THF/hexane, and analysis of these by X-ray diffraction revealed that **9** did indeed crystallize with two molecules of THF bound to the zinc center with the NTf₂ anion well separated (the cationic portion of this salt is termed **[9-THF₂]**⁺). The disparity between the observed solid state structures of 7-DIPP (3 coordinate with only one THF molecule binding) and IDIPP (4 coordinate at Zn with two

THF molecules binding) analogues deposited from THF is consistent with the DFT calculations on the relative energetics of a second molecule of THF binding to zinc. The enhanced steric impact of the 7-DIPP ligand relative to IDIPP is demonstrated by the lower % V_{bur} of IDIPP in $[\mathbf{9}\text{-THF}_2]^+$ (35.6%) relative to 7-DIPPZn analogues (7-DIPP analogue **8** which is also four coordinate due to NTf_2 binding bidentate has a % $V_{\text{bur}} = 47.2\%$). Therefore we attribute the observed disparity in catalytic reactivity between the 7-DIPP and IDIPP congeners to: (i) the preference for different coordination numbers at zinc when ligated by IDIPP (coordination number 4) Vs 7-DIPP (coordination number of 3); (ii) the greater thermal stability of the 7-DIPP species, such as **8**, **11** and **12**, relative to their IDIPP congeners (the IDIPP congeners are observed to more rapidly form insoluble species in the presence of HBPIn, presumably ZnH_2 and/or metallic zinc, during catalytic reactions) enabling superior catalyst longevity.

Conclusions

The viability of Zn-C / H-BPin σ -bond metathesis for sp , sp^2 and sp^3 C centers has been demonstrated. This step allows for zinc hydride complexes to be utilized in catalytic borylation reactions. This has been exemplified herein by developing zinc-hydrides that enable both the C-H borylation of terminal alkynes and the hydroboration of internal alkynes using the commercial borane HBPIn. The latter reaction can proceed via an uncatalyzed alkyne hydrozincation. The two borylation processes can be combined to generate a one-pot zinc catalyzed transformation of terminal alkynes that selectively produces the desirable 1,1-diborylated alkene products. This process represents an earth abundant base metal alternative to the established catalytic routes to 1,1-diborylated alkenes (these all currently rely on noble or Co transition metal catalysis both metals that have extremely low permitted daily exposure values in contrast to zinc).⁹ Mechanistic studies and DFT calculations support the intermediacy of organozinc species, zinc-hydrides and Zn-C/H-B σ -bond metathesis in both these catalytic processes. Finally, extremely bulky *N*-heterocyclic carbenes are vital for these borylation reactions, a phenomenon attributable to the larger NHC providing enhanced thermal stability and access to low (three) coordinate (NHC)Zn cations. Highly electrophilic yet Brønsted basic low coordinate, (NHC)Zn-H catalysts offer significant potential for developing new catalytic transformations a number of which are currently under development in our laboratory.

ASSOCIATED CONTENT

Supporting Information. The Supporting Information listed below is available free of charge on the ACS Publications website at DOI:

Synthetic methods and characterization details (.PDF), Crystallographic data (.cif).

AUTHOR INFORMATION

Corresponding Author

*E-mail for M.J.I.: michael.ingleson@edinburgh.ac.uk.

ORCID

Michael J. Ingleson: 0000-0001-9975-8302
Marina Uzelac: 0000-0002-5060-7017

Author Contributions

All authors have given approval to the final version of the manuscript. §RJP and MU contributed equally to the experimental sections of this work while JC performed the DFT calculations

Funding Sources

EPSRC and GSK (Case Award to RJP)
European Research Council (769599)

Notes

The authors declare no competing financial interest.

ACKNOWLEDGMENT

This work was made possible by financial support from the EPSRC and GSK (Case Award to RJP) and the Horizon 2020 Research and Innovation Program (Grant no. 769599). Prof. Richard Layfield is thanked for useful discussions.

REFERENCES

- (1) (a) Miyaura, N.; Suzuki, A. Palladium-Catalyzed Cross-Coupling Reactions of Organoboron Compounds. *Chem. Rev.* **1995**, *95*, 2457-2483. (b) Ed. Hall, D. Boronic Acids: Preparation and Applications, Wiley-VCH, **2011**. (c) Schneider, N.; Lowe, M. D.; Sayle, R. A.; Tarselli, M. A.; Landrum, G. A. Big Data from Pharmaceutical Patents: A Computational Analysis of Medicinal Chemists' Bread and Butter. *J. Med. Chem.*, **2016**, *59*, 4385-4402.
- (2) Ed. Coca, A. Boron Reagents in Synthesis, Oxford University Press, **2018**.
- (3) (a) Mkhaliid, I. A. I.; Barnard, J. H.; Marder, T. B.; Murphy, J. M.; Hartwig, J. F. C-H Activation for the Construction of C-B Bonds. *Chem. Rev.*, **2010**, *110*, 890-931; (b) Hartwig, J. F. Borylation and Silylation of C-H Bonds: A Platform for Diverse C-H Bond Functionalizations. *Acc. Chem. Res.* **2012**, *45*, 864-873; (c) Xu, L.; Wang, G.; Zhang, S.; Wang, H.; Wang, L.; Liu, L.; Jiao, J.; Li, P. Recent advances in catalytic C-H borylation reactions. *Tetrahedron*, **2017**, *73*, 7123-7157.
- (4) (a) Chirik, P.; Morris, R. Getting Down to Earth: The Renaissance of Catalysis with Abundant Metals. *Acc. Chem. Res.* **2015**, *48*, 2495-2495 (and articles contained in this special issue). (b) Enthaler, S. Rise of the Zinc Age in Homogeneous Catalysis? *ACS Catalysis*, **2013**, *3*, 150-158. (c) Hayler, J. D.; Leahy, D. K.; Simmons, E. M. A Pharmaceutical Industry Perspective on Sustainable Metal Catalysis. *Organometallics* **2018**, DOI: 10.1021/acs.organomet.8b00566.
- (5) Select examples of base metal catalysed hydroboration: (a) Bismuto, A.; Cowley, M. J.; Thomas, S. P. Aluminum-Catalyzed Hydroboration of Alkenes. *ACS Catal.* **2018**, *8*, 2001-2005. (b) Pollard, V. A.; Fuentes, M. Á.; Kennedy, A. R.; McLellan, R.; Mulvey, R. E. Comparing Neutral (Monometallic) and Anionic (Bimetallic) Aluminum Complexes in Hydroboration Catalysis: Influences of Lithium Cooperation and Ligand Set. *Angew. Chem., Int. Ed.* **2018**, *57*, 10651-10655. (c) Yang, Z.; Zhong, M.; Ma, X.; Nijesh, K.; De, S.; Parameswaran, P.; Roesky, H. W. An Aluminum Dihydride Working as a Catalyst in Hydroboration and Dehydrocoupling. *J. Am. Chem. Soc.* **2016**, *138*, 2548-2551. (d) Franz, D.; Sirtl, L.; Pöthig, A.; Inoue, S. Aluminum Hydrides Stabilized by *N*-Heterocyclic Imines as Catalysts for Hydroborations with Pinacolborane. *Z. Anorg. Allg. Chem.* **2016**, *642*, 1245-1250. (e) Nakajima, K.; Kato, T.; Nishibayashi, Y. Hydroboration of Alkynes Catalyzed by Pyrrolide-Based PNP Pincer-Iron Complexes. *Org. Lett.* **2017**, *19*, 4323-4326. (f) Romero, E. A.; Jazzar, R.; Bertrand, G. (CAAC)CuX-catalyzed hydroboration of terminal alkynes with pinacolborane directed by the X-ligand. *J. Organomet. Chem.* **2017**, *829*, 11-13. (g) Ben-Daat, H.; Rock, C. L.; Flores, M.; Groy, T. L.; Bowman, A. C.; Trovitch, R. J. Hydroboration of alkynes and nitriles using an α -diimine cobalt hydride catalyst. *Chem. Commun.* **2017**, *53*, 7333-7336. (h) Palmer, W. N.; Diao, T.; Pappas, I.; Chirik, P. J. High-Activity Cobalt Catalysts for Alkene Hydroboration with Electronically Responsive Terpyridine and α -Diimine Ligands. *ACS Catal.* **2015**, *5*, 622-626. (i) Zhang, G.; Wu, J.; Zeng, H.; Neary, M.

- C.; Devany, M.; Zheng, S.; Dub, P. A. Dearomatization and Functionalization of Terpyridine Ligands Leading to Unprecedented Zwitterionic Meisenheimer Aluminum Complexes and Their Use in Catalytic Hydroboration. *ACS Catal.* **2019**, *9*, 874–884. (j) For Cu catalyzed hydroboration see (and references therein): Xi, Y.; Hartwig, J. F.; Mechanistic Studies of Copper-Catalyzed Asymmetric Hydroboration of Alkenes. *J. Am. Chem. Soc.* **2017**, *139*, 12758–12772 (k) Mandal, S.; Verma, P. K.; Geetharani, K. Lewis acid catalysis: regioselective hydroboration of alkynes and alkenes promoted by scandium triflate. *Chem Commun.* **2018**, *54*, 13690–13693. (l) For borane catalyzed hydroboration see (and references therein): Carden, J. L.; Gierlich, L. J.; Wass, D. F.; Browne, D. L.; Melen, R. L.; Unlocking the catalytic potential of tris(3,4,5-trifluorophenyl)borane with microwave irradiation. *Chem. Commun.* **2019**, *55*, 318–321.
- (6) For select examples of base metal catalyzed (directing group free) C–H borylation see: (a) Hatanaka, T.; Ohki, Y.; Tatsumi, K. C–H Bond Activation/Borylation of Furans and Thiophenes Catalyzed by a Half-Sandwich Iron N-Heterocyclic Carbene Complex. *Chem. Asian J.* **2010**, *5*, 1657–1666. (b) Dombay, T.; Werncke, C. G.; Jiang, S.; Grellier, M.; Vendier, L.; Bontemps, S.; Sortais, J. B.; Sabo-Etienne, S.; Darcel, C. Iron Catalyzed C–H Borylation of Arenes. *J. Am. Chem. Soc.* **2015**, *137*, 4062–4065. (c) Mazzacano, T. J.; Mankad, N. P. Thermal C–H Borylation Using a CO-free Iron Boryl Complex. *Chem. Commun.* **2015**, *51*, 5379–5382. (d) Obligacion, J. V.; Semproni, S. P.; Chirik, P. J. Cobalt-Catalyzed C–H Borylation. *J. Am. Chem. Soc.* **2014**, *136*, 4133–4136. (e) For other references on advances in cobalt catalyzed borylation see (and references therein): Li, H.; Obligacion, J. V.; Chirik, P. J.; Hall, M. B. Cobalt Pincer Complexes in Catalytic C–H Borylation: The Pincer Ligand Flips Rather Than Dearomatizes. *ACS Catalysis*, **2018**, *8*, 10606–10618. (f) Furukawa, T.; Tobisu, M.; Chatani, N. Nickel-Catalyzed Borylation of Arenes and Indoles via C–H Bond Cleavage. *Chem. Commun.* **2015**, *51*, 6508–6511. (g) Romero, E. A.; Jazzar, R.; Bertrand, G. Copper-catalyzed dehydrogenative borylation of terminal alkynes with pinacolborane. *Chem. Sci.* **2017**, *8*, 165–168. (h) Wei, D.; Carboni, B.; Sortais, J.-B.; Darcel, C. Iron-Catalyzed Dehydrogenative Borylation of Terminal Alkynes. *Adv. Synth. Catal.* **2018**, *360*, 3649–3654. (i) For an example of metal free (borane) catalyzed C–H borylation see: Légaré, M. A.; Courtemanche, M. A.; Rochette, E.; Fontaine, F. G. Metal-free Catalytic C–H Bond Activation and Borylation of Heteroarenes. *Science* **2015**, *349*, 513–516. (j) For other examples of borane catalyzed C–H borylation see (and references therein) see: Zhong, Q.; Qin, S.; Yin, Y.; Hu, Y.; Hu, J.; Zhang, H. Boron(III)-Catalyzed C2-Selective C–H Borylation of Heteroarenes. *Angew. Chem. Int. Ed.*, **2018**, *57*, 14891–14895.
- (7) (a) Lee, C.-I.; Shih, W.-C.; Zhou, J.; Reibenspies, J. H.; Ozerov, O. V. Synthesis of Triborylalkenes from Terminal Alkynes by Iridium-Catalyzed Tandem C–H Borylation and Diboration. *Angew. Chem. Int. Ed.* **2015**, *54*, 14003–14007. (b) Krautwald, S.; Bezdek, M. J.; Chirik, P. J. Cobalt-Catalyzed 1,1-Diboration of Terminal Alkynes: Scope, Mechanism, and Synthetic Applications. *J. Am. Chem. Soc.* **2017**, *139*, 3868–3875.
- (8) Royes, J.; Cuenca, A. B.; Fernandez, E. Access to 1,1-Diborylalkenes and Concomitant Stereoselective Reactivity. *Eur. J. Org. Chem.* **2018**, 2728–2739.
- (9) For toxicity classification/limits set by the European Medicines Agency see: https://www.ema.europa.eu/documents/scientific-guideline/international-conference-harmonisation-technical-requirements-registration-pharmaceuticals-human-use_en-21.pdf
- (10) These base metals include Fe and Zn for which permitted daily exposure limits have not been defined due to their low toxicity, see reference 9.
- (11) McGough, J. S.; Cid, J.; Ingleson, M. J. Catalytic Electrophilic C–H Borylation Using NHC-Boranes and Iodine Forms C2-, not C3-, Borylated Indoles. *Chem. Eur. J.*, **2017**, *23*, 8180–8184
- (12) (a) Dunsford, J. J.; Clark, E. R.; Ingleson, M. J. Direct C(sp²)-C(sp³) Cross-Coupling of Diaryl Zinc Reagents with Benzylic, Primary, Secondary, and Tertiary Alkyl Halides. *Angew. Chem. Int. Ed.* **2015**, *54*, 5688–5692. (b) Procter, R. J.; Dunsford, J. J.; Rushworth, P. J.; Hulcoop, D. G.; Layfield, R. A.; Ingleson, M. J. A Zinc Catalyzed C(sp³)-C(sp²) Suzuki-Miyaura Cross-Coupling Reaction Mediated by Aryl Zincates. *Chem. Eur. J.* **2017**, *23*, 15889–15893.
- (13) (a) Tsuchimoto, T.; Utsugi, H.; Sugiura, T.; Horio, S. Alkynylboranes: A Practical Approach by Zinc-Catalyzed Dehydrogenative Coupling of Terminal Alkynes with 1,8-Naphthalenediiminatoborane. *Adv. Synth. Catal.* **2015**, *357*, 77–82. It should be noted that a combined C–X/C–H borylation catalyzed by a zinc complex has also been reported see: (b) Bose, S. K.; Deissenberger, A.; Eichhorn, A.; Steel, P. G.; Lin, Z.; Marder, T. B. Zinc-Catalyzed Dual C–X and C–H Borylation of Aryl Halides. *Angew. Chem. Int. Ed.*, **2015**, *54*, 11843–11847.
- (14) For recent reviews see: (a) Wiegand, A.-K.; Rit, A.; Okuda, J. Molecular zinc hydrides. *Coord. Chem. Rev.*, **2016**, *314*, 71–82; and (b) Dargone, S.; Recent Developments on N-Heterocyclic Carbene Supported Zinc Complexes: Synthesis and Use in Catalysis. *Synthesis* **2018**, *50*, 3662–3670. (c) Butler, M. J.; Crimmin, M. R. Magnesium, zinc, aluminium and gallium hydride complexes of the transition metals. *Chem. Commun.* **2017**, *53*, 1348–1365. For select recent papers on ligated zinc-hydrides/alkyls see: (d) Rit, A.; Zanardi, A.; Spaniol, T. P.; Maron, L.; Okuda, J. A Cationic Zinc Hydride Cluster Stabilized by an N-Heterocyclic Carbene: Synthesis, Reactivity, and Hydrosilylation Catalysis. *Angew. Chem. Int. Ed.* **2014**, *53*, 13273–13277. (e) Lummis, P. A.; Momeni, M. R.; Lui, M. W.; McDonald, R.; Ferguson, M. J.; Miskolzie, M.; Brown, A.; Rivard, E. Accessing Zinc Monohydride Cations through Coordinative Interactions. *Angew. Chem. Int. Ed.* **2014**, *53*, 9347–9351. (f) Lortie, J. L.; Dudding, R.; Gabidullin, B. M.; Nikonov, G. I. Zinc-Catalyzed Hydrosilylation and Hydroboration of N-Heterocycles. *ACS Catal.* **2017**, *7*, 8454–8459. (g) Specklin, D.; Hild, F.; Fliedel, C.; Gourlaouen, Veiros, L. F.; Dargone, S. Accessing Two-Coordinate Zn^{II} Organocations by NHC Coordination: Synthesis, Structure, and Use as p-Lewis Acids in Alkene, Alkyne, and CO₂ Hydrosilylation. *Chem. Eur. J.* **2017**, *23*, 15908–15912.
- (15) Clary, J. W.; Rettenmaier, T. J.; Snelling, R.; Bryks, W.; Banwell, J.; Wipke, T.; Singaram, B. Hydride as a Leaving Group in the Reaction of Pinacolborane with Halides under Ambient Grignard and Barbier Conditions. One-Pot Synthesis of Alkyl, Aryl, Heteroaryl, Vinyl, and Allyl Pinacolboronic Esters. *J. Org. Chem.* **2011**, *76*, 9602–9610
- (16) Dunsford, J. J.; Evans, D. J.; Pugh, T.; Shah, S. N.; Chilton, N. F.; Ingleson, M. J. Three-Coordinate Iron(II) Expanded Ring N-Heterocyclic Carbene Complexes. *Organometallics*, **2016**, *35*, 1098–1106.
- (17) Naumann, S.; Schmidt, F. G.; Frey, W. Protected N-heterocyclic carbenes as latent pre-catalysts for the polymerization of 3-caprolactone. *Polym. Chem.*, **2013**, *4*, 4172
- (18) Collins, L. R.; Moffat, L. A. Mahon, M. F.; Jones, M. D.; Whittlesey, M. K. Lactide polymerisation by ring-expanded NHC complexes of zinc. *Polyhedron*, **2016**, *103*, 121–125.
- (19) (a) Frey, G. D.; Masuda, J. D.; Donnadiu, B.; Bertrand, G. Activation of Si–H, B–H, and P–H Bonds at a Single Nonmetal Center. *Angew. Chem. Int. Ed.* **2010**, *49*, 9444–9447. (b) Würtemberger-Pietsch, S.; Schneider, H.; Marder, T. B.; Radius, U. Adduct Formation, B–H Activation and Ring Expansion at Room Temperature from Reactions of HBcat with NHCs. *Chem. Eur. J.*, **2016**, *22*, 13032–13036.
- (20) Rit, A.; Spaniol, T. P.; Maron, L.; Okuda, J. Molecular Zinc Dihydride Stabilized by N-Heterocyclic Carbenes. *Angew. Chem. Int. Ed.* **2013**, *52*, 4664–4667.
- (21) (a) Gutschank, B.; Schulz, S.; Bläser, Boese, R.; Wölper, C. Synthesis, Structure, and Reactivity of a Tetranuclear Amidinato Zinc Hydride Complex. *Organometallics* **2010**, *29*, 6133–6136. (b) Han, R.; Gorrell, I. B.; Looney, A. G.; Parkin, G. Tris(3-tert-butylpyrazolyl)hydroborato Zinc Hydride: Synthesis, Structure and Reactivity of a Monomeric Zinc Hydride Derivative. *J. Chem. Soc., Chem. Commun.*, **1991**, 717–718.
- (22) Jiao, J.; Nishihara, Y. Alkynylboron compounds in organic synthesis. *J. Organomet. Chem.* **2012**, *721*–722, 3–16.
- (23) (a) Nagashima, Y.; Takita, R.; Yoshida, K.; Hirano, K.; Uchiyama, M. Design, Generation, and Synthetic Application of Borylzincate: Borylation of Aryl Halides and Borylzincation of Benzyne/Terminal Alkyne. *J. Am. Chem. Soc.* **2013**, *135*, 18730–18733. (b) Nagashima, Y.; Yukimore, D.; Wang, C.; Uchiyama, M. In Situ Generation of Silylzinc by Si–B Bond Activation Enabling Silylzincation and Silaboration of Terminal Alkynes. *Angew. Chem. Int. Ed.*, **2018**, *57*, 8053–8057.
- (24) To the best of our knowledge all previously reported alkyne hydrozincation reactions are catalyzed by transition metals, for example:

- (a) Vettel, S.; Vaupel, A.; Knochel, P. A new preparation of diorganozincs from olefins via a nickel catalyzed hydrozincation. *Tett. Lett.* **1995**, 36, 1023-1026. (b) Gao, Y.; Harada, K.; Hata, T.; Urabe, H.; Sato, F. Stereo- and Regioselective Generation of Alkenylzinc Reagents via Titanium-Catalyzed Hydrozincation of Internal Acetylenes. *J. Org. Chem.*, **1995**, 60, 290-291. In a recent review on hydrometallation see: Chen, J.; Guo, J.; Lu, Z. Recent advances in the hydrometallation of alkenes and alkynes. *Chin. J. Chem.* **2018**, 36, 1075–1109, zinc catalysis of alkyne hydrosilylation was reported but as discussed in ref. 14g this is not proposed to proceed by hydrozincation but instead by zinc activation of H-SiR₃ generating a silicon electrophile that reacts with the alkyne (analogous to the reactivity of B(C₆F₅)₃ with silanes / alkynes).
- (25) Zhao, F.; Jia, X.; Li, P.; Zhao, J.; Zhou, Y.; Wang, J.; Liu, H. Catalytic and catalyst-free diboration of alkynes. *Org. Chem. Front.* **2017**, 4, 2235
- (26) Morinaga, A.; Nagao, K.; Ohmiya, H.; Sawamura, M. Synthesis of 1,1-Diborylalkenes through a Brønsted Base Catalyzed Reaction between Terminal Alkynes and Bis(pinacolato)diboron. *Angew. Chem. Int. Ed.* **2015**, 54, 15859
- (27) For borane catalyzed hydroboration see (and references therein): (a) Nag, N. W. J.; Buettner, C. S.; Docherty, S.; Bismuto, A.; Carney, J. R.; Docherty, J. H.; Cowley, M. J.; Thomas, S. P. Borane Catalysed Hydroboration of Alkynes and Alkenes. *Synthesis*, **2018**, 50, 803–808. For a recent example see of “Trojan horse” metal initiated borane catalyzed hydroboration see: (b) Harder, S.; Spielmann, J. Calcium-mediated hydroboration of alkenes: “Trojan horse” or “true” catalysis? *J. Organomet. Chem.* **2012**, 698, 7-14.
- (28) Jochmann, P.; Stephan, D. W.; Reactions of CO₂ with Heteroleptic Zinc and Zinc–NHC Complexes. *Organometallics* **2013**, 32, 7503–7508
- (29) Roberts, A. J.; Clegg, W.; Kennedy, A. R.; Probert, M. R.; Robertson, S. D.; Hevia, E. Two alternative approaches to access mixed hydride-amido zinc complexes: synthetic structural and solution implications. *Dalton Trans.* **2015**, 44, 8169.
- (30) For a select example see: Dawkins, M. J. C.; Middleton, E.; Kefalidis, C. E.; Dange, D.; Juckel, M. M.; Maron, L.; Jones, C. Two-coordinate terminal zinc hydride complexes: synthesis, structure and preliminary reactivity studies. *Chem. Commun.*, **2016**, 52, 10490
- (31) Hall, J. W.; Unson, D. M. L.; Brunel, P.; Collins, L. R.; Cybulski, M. K.; Mahon, M. F.; Whittlesey, M. K. Copper-NHC-Mediated Semi-hydrogenation and Hydroboration of Alkynes: Enhanced Catalytic Activity Using Ring-Expanded Carbenes. *Organometallics* **2018**, 37, 3102–3110.
- (32) The mono-THF solvate is used throughout for DFT calculations, including for the hydrozincation reactions. For reactions performed in benzene a THF solvate is clearly not feasible, however, the THF solvate still is used to keep the model constant throughout and to simplify the calculations (if THF is replaced by NTf₂ mono and bidentate NTf₂ binding modes need to be considered for all steps). It should be noted that all the energies obtained using this model correlate well with the observed solution reactivity.
- (33) Wang, J. Y.; Zheng, W. R.; Ding L. L.; Wang Y. X. Computational study on C–B homolytic bond dissociation enthalpies of organoboron compounds. *New. J. Chem.*, **2017**, 41, 1346-1362.
- (34) Rablen, P. R.; Hartwig J. F.; Accurate Borane Sequential Bond Dissociation Energies by High-Level ab Initio Computational Methods. *J. Am. Chem. Soc.* **1996**, 118, 19, 4648-4653.

